A sensitized mutagenesis screen in Factor V Leiden mice identifies novel thrombosis suppressor loci

Randal J. Westrick[1,2,3,*], Kärt Tomberg[3,4,*], Amy E. Siebert[1], Guojing Zhu[3], Mary E. Winn[3], Sarah L. Dobies[3], Sara L. Manning[3], Marisa A. Brake[1], Audrey Cleuren[3], Lena M. Mishack[1], Linzi M. Hobbs[1], Alexander Johnston[1], David R. Siemieniak[5], Jishu Xu[4], Jun Z. Li[4] and David Ginsburg[3,4,5,6]

[1]Oakland University Department of Biological Sciences

[2]Oakland University Center for Data Science and Big Data Analysis

[3]Life Sciences Institute, University of Michigan

[4]Department of Human Genetics, University of Michigan

[5]Howard Hughes Medical Institute

[6]Departments of Internal Medicine and Pediatrics, University of Michigan

*These authors contributed equally to this work

Co-corresponding authors:

David Ginsburg, MD. 5214 LSI Building, 210 Washtenaw Avenue, Ann Arbor MI 48109. E-mail: ginsburg@umich.edu, Telephone: 734-647-4808, Fax: 734-936-2888.

Randal Westrick, PhD. 1800 Library Drive, 305 Dodge Hall, Rochester MI, 48309-4479 E-mail: rjwestrick@oakland.edu, Telephone: 248-370-3577.

Abstract

Factor V Leiden ($F5^{L}$) is a common genetic risk factor for venous thromboembolism (VTE), though it exhibits only 10% penetrance. We conducted a sensitized ENU mutagenesis screen for dominant thrombosuppressor genes based on perinatal lethal thrombosis in mice homozygous for $F5^{L}$ ($F5^{L/L}$) and haploinsufficient for tissue factor pathway inhibitor ($Tfpi^{+/-}$). The observation that *F8* deficiency enhanced survival of $F5^{L/L}$ $Tfpi^{+/-}$ mice demonstrated the potential for genetic suppression of $F5^{L/L}$ $Tfpi^{+/-}$ lethality. G0 ENU-mutagenized $F5^{L/L}$ males and $F5^{L/+}$ $Tfpi^{+/-}$ females were next crossed to generate 6,739 G1 progeny, with 98 $F5^{L/L}$ $Tfpi^{+/-}$ offspring surviving until weaning and 16 exhibiting transmission of a putative thrombosuppressor to subsequent generations. The resulting lines are referred to as *MF5L,* (**M**odifier of **F**actor **5** **L**eiden 1-16). Linkage analysis in *MF5L6* identified a chromosome 3 locus containing the tissue factor gene (*F3*). Though no ENU-induced *F3* mutation was identified, heterozygous *F3* deficient mice ($F3^{+/-}$) suppressed $F5^{L/L}$ $Tfpi^{+/-}$ lethality. Thus, like *F8* deficiency, reduced *F3* activity suppresses $F5^{L/L}$ $Tfpi^{+/-}$ thrombosis. Whole exome sequencing in *MF5L12* identified an *Actr2* gene point mutation (p.R258G) as the sole candidate. Attempts to generate an independent *Actr2* knockin/knockout via CRISPR/Cas9 failed for any mouse beyond the 60-cell stage. Our findings identify *F8* and the *TFPI/F3* axis as key regulators of thrombosis balance in the setting of $F5^{L}$ and demonstrate the utility of this sensitized ENU mutagenesis approach for the identification of dominant thrombosis suppressor loci.

Introduction

Venous thromboembolism (VTE) is a common disease that affects 1 to 3 per 1000 individuals per year[1]. VTE susceptibility exhibits a complex etiology involving contributions of both genes and environment. Genetic risk factors explain approximately 60% of the overall risk for VTE[2]. Recent large-scale genome wide association studies (GWAS) confirm *ABO*, *F5*, *FGG* and *F2* as thrombosis susceptibility genes, with few additional novel loci identified[3-5], leaving the major component of VTE genetic risk still unexplained.

The Factor V Leiden variant ($F5^L$) is a common inherited risk factor for VTE with an allele frequency of 2-10% in most European-derived populations[6, 7]. $F5^L$ is estimated to account for up to 25% of the genetically-attributable thrombosis risk in humans[6]. However, penetrance is incomplete, with only 10% of $F5^L$ heterozygotes developing thrombosis in their lifetimes. The severity of thrombosis also varies widely among affected individuals[7, 8], limiting the clinical utility of $F5^L$ genotyping in the management of VTE[9].

The incomplete penetrance and variable expressivity of thrombosis among $F5^L$ patients can at least partially be explained by genetic interactions between $F5^L$ and other known thrombotic risk factors such as hemizygosity for antithrombin III or proteins C or S, as well as the common prothrombin 20210 polymorphism[8, 10, 11]. However, <2% of $F5^L$ heterozygotes would be expected to co-inherit a mutation at one or more of these loci, suggesting that a large number of additional genetic risk factors for VTE and/or modifiers of $F5^L$ remain to be identified[3, 8].

Mice carrying the orthologous $F5^L$ mutation exhibit a mild to moderate prothrombotic phenotype closely mimicking the human disorder[12]. We previously reported a synthetic lethal interaction between $F5^L$ homozygosity ($F5^{L/L}$) and hemizygosity for tissue factor pathway

inhibitor (*Tfpi*$^{+/-}$)[13]. Nearly all mice with this lethal genotype combination (*F5*$^{L/L}$ *Tfpi*$^{+/-}$) succumb to widespread, systemic thrombosis in the immediate perinatal period[13].

ENU mutagenesis in mice has been used effectively to identify novel genes involved in a number of biological processes[14, 15]. ENU-induced germline mutations transmitted from a mutagenized male mouse (G0) occur at ~1.5 mutations per megabase, at least 50 fold higher than the endogenous background mutation rate[16]. Several previous reports have successfully applied an existing phenotype as a sensitizer to identify modifier genes. A dominant suppressor screen in *MecP2* deficient mice (Rett syndrome) identified a mutation in squalene epoxidase (*Sqle)* as a heritable suppressor, resulting in prolonged survival and amelioration of neurologic manifestations[17]. Other successful sensitized screens include analysis of mouse mutants predisposed to diabetic nephropathy[18], a screen in *Sox10* haploinsufficent mice identifying the *Gli3* gene as a modifier of neurochristopathy[19] and identification of a mutation in the *c-Myb* gene as a dominant modifier for platelet count in *Mpl* deficient mice (congenital thrombocytopenia)[20].

We now report the results of a dominant, sensitized ENU mutagenesis screen for suppressors of *F5*$^{L/L}$ *Tfpi*$^{+/-}$ dependent lethal thrombosis.

Results and Discussion

F8 deficiency suppresses *F5*$^{L/L}$ *Tfpi*$^{+/-}$ lethality

To test whether the *F5*$^{L/L}$ *Tfpi*$^{+/-}$ lethal phenotype was genetically suppressible by *F8* deficiency (X-linked hemophilia A in humans), triple heterozygous *F5*$^{L/+}$ *Tfpi*$^{+/-}$ *F8*$^{+/-}$ female mice were generated and crossed to *F5*$^{L/L}$ male mice (Figure 1A). One quarter of conceptuses are expected to carry the *F5*$^{L/L}$ *Tfpi*$^{+/-}$ genotype, with half of the total expected male conceptuses completely *F8* deficient (*F8*$^{-}$), and thus 1/16th of the overall offspring from this mating expected

to be $F5^{L/L}$ $Tfpi^{+/-}$ $F8^{-}$ (males). Similarly, 1/16th of the progeny should be $F5^{L/L}$ $Tfpi^{+/-}$ $F8^{+/-}$ (females). A total of 167 progeny from this cross were genotyped at weaning, with 8 $F5^{L/L}$ $Tfpi^{+/-}$ $F8^{-}$ male mice observed (compared to 0 $F5^{L/L}$ $Tfpi^{+/-}$ $F8^{+}$, p=0.01) and 2 $F5^{L/L}$ $Tfpi^{+/-}$ $F8^{+/-}$ female mice (compared to 1 $F5^{L/L}$ $Tfpi^{+/-}$ $F8^{+/+}$, N.S.) (Sup. Table 1). These data strongly suggest that the $F5^{L/L}$ $Tfpi^{+/-}$ phenotype is genetically suppressible and are consistent with human studies demonstrating *F8* level as an important VTE risk factor[21].

The $F5^{L/L}$ $Tfpi^{+/-}$ phenotype is suppressed by dominant ENU induced mutations

A sensitized, genome-wide ENU mutagenesis screen for dominant thrombosis suppressor genes was implemented as depicted in Figure 1B. ENU mutagenized G0 $F5^{L/L}$ males were crossed to $F5^{L/+}$ $Tfpi^{+/-}$ females to generate G1 mice, which were screened by genotyping at weaning for $F5^{L}$ and $Tfpi^{+/-}$. Previously described visible dominant mutants[22], including belly spotting and skeletal abnormalities, were observed in approximately 5.9% of G1 offspring, similar to the ~4.2% rate of observable mutants in previous studies[22], and consistent with the ~20-30 functionally significant mutations per G1 mouse expected with this ENU mutagenesis protocol[23, 24]. One quarter of G1 embryos from this cross would be expected to carry the synthetic lethal $F5^{L/L}$ $Tfpi^{+/-}$ genotype. Out of a total of 6,739 G1 mice screened at weaning, the 98 live $F5^{L/L}$ $Tfpi^{+/-}$ mice (45 females, 53 males, Sup. Table 2) represented 4.4% of the 2,214 embryos expected with this genotype.

The heritability of each of the 98 G1 putative suppressor mutants was evaluated by a progeny test backcross to C57BL/6J (B6) $F5^{L/L}$ mice. The observation of one or more $F5^{L/L}$ $Tfpi^{+/-}$ offspring surviving to weaning increased the likelihood that a particular modifier of Factor 5 Leiden (*MF5L*) line carries a transmissible suppressor mutation. 75 of the 98 surviving $F5^{L/L}$ $Tfpi^{+/-}$ G1 mice produced no offspring surviving to weaning, either due to early lethality or

infertility, with over 1/2 of these mice (37 of 75) exhibiting a grossly runted appearance. Survival data were available for 57 of the $F5^{L/L}$ $Tfpi^{+/-}$ G1 mice, with 34 living past 70 days of age with a trend toward poorer survival for females (Figure 1C). Of the 23 $F5^{L/L}$ $Tfpi^{+/-}$ G1 mice producing 1 or more G2 progeny surviving to weaning, 7 produced no $F5^{L/L}$ $Tfpi^{+/-}$ G2s, including 4 G1s with 8 or more offspring of other genotypes. Sixteen $F5^{L/L}$ $Tfpi^{+/-}$ G1 mice (4 female, 12 male) produced one or more $F5^{L/L}$ $Tfpi^{+/-}$ progeny when bred to B6 $F5^{L/L}$ mice (Sup Table 3). These 16 putative "rescue" mice were crossed into 129S1/SvIMJ (129S1) to generate suppressor lines of genetically informative progeny for genetic mapping. The number of total progeny, genotypic distribution and penetrance of the $F5^{L/L}$ $Tfpi^{+/-}$ mice in each line are listed in Sup. Table 3. Within these suppressor lines, mice with the $F5^{L/L}$ $Tfpi^{+/-}$ genotype were ~30% smaller than their $F5^{L/L}$ littermates at the time of weaning ($p<2.2x10^{-16}$, Figure 1D), with this difference maintained after outcrossing to the 129S1 strain (Figure 1E).

Previous reports based on the specific locus test estimate an ENU-induced mutation rate of 1/700 visible mutations per locus for the ENU dosing regimen used here[28]. This mutation rate predicts that our screen of 6,739 G1 progeny (2214 $F5^{L/L}$ $Tfpi^{+/-}$ expected) should have resulted in ~3 mutations per gene averaged over the entire genome, with 54% of these mutations expected to be null based on gene function in a specific locus test (28), for an overall estimated genome coverage with null mutations of ~1.5X.

The *MF5L6* suppressor mutation maps to a chromosome 3 interval containing *F3*

In order to map putative ENU-induced suppressor mutations, surviving $F5^{L/L}$ $Tfpi^{+/-}$ mice were intercrossed with $F5^{L/L}$ mice that had been extensively backcrossed onto the 129S1 strain. Crosses between $F5^{L/L}$ and $F5^{L/+}$ $Tfpi^{+/-}$ mice (both $F5^{L}$ and $Tfpi^{-}$ backcrossed > 12 generations

onto 129S1) confirmed the lethality of the $F5^{L/L}$ $Tfpi^{+/-}$ genotype on the 129S1 background (Sup. Table 4).

Each *MF5L* suppressor line was intercrossed to 129S1 mice, with the 4 largest lines (*MF5L1, 6, 9* and *16*) producing greater than 13 surviving $F5^{L/L}$ $Tfpi^{+/-}$ offspring on the mixed 129S1-B6 genetic background. Though the *MF5L1*, *MF5L9* and *MF5L16* were successfully expanded to pedigrees containing 27, 84, and 14 $F5^{L/L}$ $Tfpi^{+/-}$ informative offspring, respectively, genotyping for a total of ~800 markers in each cross failed to identify any loci with a LOD $\gtrsim$3 (Sup. Table 5). The absence of a clear linkage signal for each of these lines likely reflects complex mouse strain modifier gene interactions, which are known to significantly impact mouse phenotypes[8, 25] and confound linkage analysis[26]. Consistent with this hypothesis, analysis of $F5^{L/L}$ and $F5^{L/+}$ littermates demonstrated consistently poorer survival in the purebred 129S1 versus B6 strain backgrounds[12] (Sup. Table 4, Sup. Table 6).

*MF5L*6 was maintained for 12 generations on both the mixed and B6 backgrounds and produced a total of 336 $F5^{L/L}$ $Tfpi^{+/-}$ mice (98 of which were genetically heterogeneous and therefore useful for linkage analysis). Genome-wide SNP genotyping was performed on DNA from 98 genetically informative $F5^{L/L}$ $Tfpi^{+/-}$ mice, with multipoint linkage analysis shown in Figure 2A. Since the genetic intervals around the *F5* and *Tfpi* loci cannot be accurately assessed for linkage, these regions of chromosomes 1 and 2 were excluded from linkage analysis (See figure legend or Methods). A single locus with a maximum LOD score >3.3 was identified on Chr 3 (maximum LOD=4.49), with the 1 LOD interval (117.3-124.8Mb) containing 38 refseq annotated genes (Figure 2C).

The *F3* gene located at Chr3:121.7 Mb (Figure 2C) encodes Tissue factor (TF), a procoagulant component of the hemostatic pathway that has *Tfpi* as its major regulator.

Quantitative or qualitative deficiencies in *F3* are thus highly plausible candidates to suppress the $F5^{L/L}$ $Tfpi^{+/-}$ phenotype. However, analysis of sequencing data from the full set of *F3* exons and introns as well as the 5kb upstream of exon 1, failed to identify an ENU-induced mutation. Analysis of *F3* mRNA levels in liver, lung and brain tissues of adult mice failed to identify any differences in the level of expression from the ENU-mutant compared to the wildtype allele (Sup. Fig 1). However, an ENU-induced regulatory mutation outside the sequenced region that confers a key change in tissue- or developmental stage-specific F3 mRNA expression, or in response to environmental stress, cannot be excluded.

Whole exome sequencing data analysis of a $F5^{L/L}$ $Tfpi^{+/-}$ mouse from *MF5L6* (see below) failed to identify an ENU variant in *F3* or the other genes on chromosome 3. Although additional ENU variants were identified on other chromosomes, none co-segregated with the survival phenotype in line *MF5L6* (Sup. Table 8).

_F3_ haploinsufficiency suppresses the $F5^{L/L}$ $Tfpi^{+/-}$ lethal phenotype

To test *F3* as a candidate suppressor of the $F5^{L/L}$ $Tfpi^{+/-}$ phenotype, an independent *F3* null allele was introduced and triply heterozygous $F5^{L/+}$ $Tfpi^{+/-}$ $F3^{+/-}$ mice crossed to $F5^{L/L}$ B6 mice (Figure 2B). Of 272 progeny genotyped at weaning, 13 $F5^{L/L}$ $Tfpi^{+/-}$ $F3^{+/-}$ were observed (compared to 1 $F5^{L/L}$ $Tfpi^{+/-}$ $F3^{+/+}$, p=0.004, Sup. Table 7). We also observed significantly fewer male than female $F5^{L/L}$ $Tfpi^{+/-}$ $F3^{+/-}$ mice (2 vs. 11 p=0.03). Thus, haploinsufficiency for $F3^{+/-}$ suppresses the synthetic lethal $F5^{L/L}$ $Tfpi^{+/-}$ phenotype, though with incomplete penetrance (33%) that also differs by gender (10% for females and 67% for males). Gender specific differences in venous thrombosis rates have previously been reported, including contributions from oral contraceptives and hormone replacement therapy[27, 28]. Conversely, the MF5L6 line had an overall penetrance of 72.4%, with similar male/female penetrance. This difference in penetrance

could be due to 129S1 strain effects in the MF5L6 line. Our Sanger sequencing data of F3 exons and regulatory regions identified no mutations. However, enhancers and repressors greater than 1 megabase away from a gene's transcription start site have been documented to control gene expression. Taken together, these data suggest that an ENU-induced *F3* regulatory mutation outside of the sequenced segment may be responsible for thrombosuppression in *MF5L6*, though we cannot exclude regulatory mutation in another gene. Nonetheless, our findings demonstrate that *F3*/*Tfpi* balance plays a key role in VTE in the mouse, particularly in the setting of $F5^{L}$, and suggest that modest variations in either *F3* or *Tfpi* could be important modifiers of VTE susceptibility in humans.

Whole exome sequencing identifies candidate ENU suppressor variants for 8 *MF5L* lines

Whole exome-next generation sequencing (NGS) was performed on genomic DNA from one $F5^{L/L}$ $Tfpi^{+/-}$ mouse of varying generations (ranging from G2 to G5), from each of 8 *MF5L* lines, including the 4 lines described above, as well as 4 additional lines with large pedigrees (*MF5L5*, *MF5L8*, *MF5L11*, *MF5L12*). The mean coverage of sequenced exomes was more than 90X, with >97% of the captured region covered with at least 6 independent reads (Sup. Table 8). A total of 125 heterozygous variants were identified as candidate suppressor mutations, with 79 variants occurring within coding sequence. Of these latter mutations, 54.5% were nonsynonymous single nucleotide variants (SNVs), followed by UTR (17.6%), synonymous (14.4%) and stopgain SNVs (7.2%), with the remainder being comprised of indels, splicing, and stoploss mutations. The most common mutation events were A/T→G/C transitions (35.2%), while C/G→G/C transversions were the least represented (2.5%). This spectrum of mutations is consistent with previously published ENU reports[29]. Validation was performed for 52 variants by Sanger sequencing, including all nonsynonymous and stopgain mutations. Variants exhibiting no

recombination with the *Tfpi* locus on chromosome 2 were excluded from further analysis (See methods of Fig 2A). The remaining variants were then checked for parent of origin (either the G1 mutagenized progeny or its nonmutagenized mate) as well as the original mutagenized G0 male. 42 of the variants were identified in the G1 mouse but not in the G0 or nonmutagenized parent, consistent with an ENU-induced mutations. The remaining 10 mutations were either not verified or were transmitted from the non-mutagenized parent, indicating either spontaneous mutations in the nonmutagenized parent or errors in the sequencing data. (Sup. Table 9).

Each SNV was analyzed for validation in additional mice *MF5L* mice from the line in which it was identified. None of the thrombosuppressive exonic ENU-induced variants were validated in lines *MF5L*1, 5, 6, 8, 11 and 16 (either they did not segregate with the lethal phenotype or they were exome sequencing errors). Of the 7 candidate ENU-induced SNVs identified from whole exome sequencing analysis for the *MF5L12* line, 6 were validated by Sanger sequencing as consistent with ENU-induced mutations in the G0 mice (Sup. Table 10). For each of these 6 SNVs, co-segregation with the survival phenotype was tested by Kaplan-Meier analysis of 31 $F5^{L/L}$ $Tfpi^{+/-}$ mice from the *MF5L12* line. Only one variant, a nonsynonymous SNV in the *Actr2* gene ($Actr2^{+/G}$), demonstrated a significant survival advantage[22] when co-inherited with the $F5^{L/L}$ $Tfpi^{+/-}$ genotype ($p=1.7x10^{-6}$) (Figure 3A).

The *Actr2* gene encodes the ARP2 protein, which is an essential component of the ARP2/3 complex[30]. The $Actr2^{+/G}$ mutation results in a p.R258G substitution in exon 7 of *Actr2*, at a highly conserved amino acid position, with arginine present at this position for all 60 available vertebrate sequences (https://genome.ucsc.edu), as well as in plants and fungi (Figure 3B). In addition, no variants at this position have been identified to date in over 120,000 human alleles (ExAC, http://exac.broadinstitute.org accessed: 10/2016). The ARP2/3 complex is

essential for actin branching and polymerization and complete ARP3 deficiency is embryonic lethal in mice[31]. The other members of the complex include ARPC 1-5. Disruption of any one of the members of the ARP2/3 complex has been demonstrated to reduce the activity of the complex[32]. ARP2 deficiency was demonstrated to influence platelet shape change, a process that is critical for normal platelet function and thus for hemostasis[33].

Complete *Actr2* deficiency is incompatible with survival

We attempted to generate an independent *Actr2* knockin (Actr2^{G}/knockout allele (*Actr2*$^{-}$) by CRISPR/Cas9 technology. We were able to detect blastocysts with our prepared CRISPR materials. We have analyzed these 13 blastocysts and have found one that harbored a homozygous C to G mutation (Sup Figure 2C, first gold arrow), as well as 3 that harbored a heterozygous C to G mutation. We have also identified our engineered homozygous synonymous G to A mutation (Sup Figure 2C, second gold arrow).

The efficiency of this strategy for establishing stable CRISPR mouse lines is high, as it was reported that for every 100 embryos that underwent pronuclear co-injection, 13.3 genetically modified embryos were produced[34]. Of the 300 embryos injected and implanted, we obtained 18 live mice, none of which had an Actr2 modification by either nonhomologous end joining (NHEJ) or homology directed repair (HDR). Since modifications have been shown to occur with high frequency[35], this suggests that *Actr2* deficiency is incompatible with survival.

We queried the components of the ARP2/3 including ARP2, ARP3 and ARPC 1-5 for loss of function mutations. ARPC1A, ARPC2, ARPC3, ARPC4, ARPC5, ARP2 and ARP3 all had a significantly reduced or absent loss of function mutations (Table 1, ExAC, http://exac.broadinstitute.org accessed: 10/2016).

Upon analysis of Neuro2A cells, we were not able to detect complete *Actr2* deficiency in any of 36 single cell colonies we successfully propagated, further suggesting that *Actr2* is incompatible with survival.

VTE susceptibility genes have been refractory to a number of methods of discovery, likely due to the incomplete penetrance and variable expressivity of VTE interposed with the significant environmental risk component. This is based on the fact that although many small and large-scale genetic studies have been performed, few novel VTE susceptibility loci have been identified[3, 36]. Given the issue of identifying "missing heritability" in human genetics studies[37], forward genetic studies using ENU mutagenesis/NGS for mutant identification can drive the discovery of novel pathways (and drug targets) contributing to disease pathology. A distinct advantage of the ENU approach over human studies is that an identified mutation will nearly always be causative, because genetically linked variants will be rare. The specific advantage of a sensitized genetic screening approach that we have adopted here means that the entire mutation space can be queried for identifying suppressors of our specific $F5^{L/L}$ $Tfpi^{+/-}$ phenotype. These types of phenotype-genotype correlations have been very difficult to form through genetic studies in humans but as described in the introduction, like our study have been successful in mice[38].

The problem of endogenous strain modifier genes interfering with ENU mutation induced phenotypes has been recognized for some time, with 50% of ENU induced phenotypes being lost upon outcrossing to a different strain to introduce the genetic diversity necessary for standard gene mapping approaches[22, 39]. Our experimental approach affirms the use of NGS for identification of ENU induced mutants by circumventing lengthy gene mapping approaches[40]

and also for enabling the identification of ENU mutants like those we have described here whose phenotype may have been obscured by "endogenous" mouse strain modifiers.

Finally and most importantly, through the design and execution of this sensitized ENU mutagenesis screen, we have identified genomic loci capable of suppressing $F5^{L/L}$ $Tfpi^{+/-}$ lethality. Specifically, our work has illustrated the importance of the TF/TFPI axis in thrombosis regulation as well as the identification of *Actr2* as a prime candidate the *MfvL*1 suppressor mutant.

Materials and methods

Mice

C57BL/6J (B6, stock number 000664), 129S1/SvImJ mice (129S1, stock number 002448), were purchased from Jackson Laboratories. $F5^{L/L}$ ($F5^{tm2Dgi}$/J stock number 004080) mice were previously generated[22]. *F3* and *Tfpi* deficient mice were a generous gift of Dr. George Broze[41, 42]. *F8* deficient mice were a generous gift of Dr. Haig Kazazian[43]. All mice designated to be on the B6 background were backcrossed greater than 8 generations to B6. $F5^{L/L}$ breeding stock for genetic mapping were generated from $F5^{L}$ mice serially backcrossed greater than 12 generations to the 129S1 strain to create $F5^{L}$ congenic mice. All mice were maintained on normal chow in a specific pathogen-free (SPF) facility. All animal care and experimental procedures complied with the principles of Laboratory and Animal Care established by the National Society for Medical Research and were approved by the University of Michigan Committee on Use and Care of Animals.

Genotyping

DNA was isolated from tail biopsies and mice genotyped for *Tfpi*$^{+/-}$ and *F5*^{L} as previously described[13]. Mice were genotyped for *F3* deficiency using custom primers listed in Sup. Table 10. All primers were purchased from IDT, Coralville, IA.

ENU mutagenesis and breeding

ENU was purchased (Sigma Aldrich, St. Louis MO) in ISOPAC vials, and prepared according to the following protocol http://pga.jax.org/enu_protocol.html. A single ENU dose of 150 mg/kg was administered intraperitoneally into an initial cohort of 159 *F5*$^{L/L}$ B6 male mice (referred to as generation 0 or G0 mice). For a second cohort of 900 male *F5*$^{L/L}$ G0 mice, the protocol was changed to three weekly intraperitoneal injections of ENU (90 mg/kg). After a 10-week recovery period, each G0 mouse was bred to *F5*$^{L/+}$ *Tfpi*$^{+/-}$ mice (Figure 1B) on the B6 genetic background to produce G1 generation offspring, which were genotyped at two weeks of age. G1 mice of the *F5*$^{L/L}$ *Tfpi*$^{+/-}$ genotype surviving to weaning age were considered to carry a suppressor mutation.

Modifier gene transmission

F5$^{L/L}$ *Tfpi*$^{+/-}$ G1 founders were crossed to *F5*$^{L/L}$ mice on the B6 genetic background to produce G2 generation offspring. G2 mice were outcrossed to *F5*$^{L/L}$ mice on the 129S1 genetic background for 2 or more generations. Progeny testing was considered positive when the identification of *F5*$^{L/L}$ *Tfpi*$^{+/-}$ offspring was greater than or equal to 2.4% of the total progeny.

Genetic Mapping

Genetic markers distinguishing the B6 and 129S1 strains distributed across the genome were genotyped using the Illumina GoldenGate Genotyping Universal-32 platform (Illumina, San Diego CA) at the University of Michigan DNA Sequencing Core. Linkage Analysis was performed on the Mendel platform version 14.0[44] using 806 informative markers from the total

of 1449 genotyped markers. LOD scores >=3.3 were considered significant[45]. The number of mice, the number of SNP markers and the LOD scores for each of the mapped pedigrees are listed in Sup. Table 5.

Sanger sequencing of the *F3* gene and analysis of candidate mutations

Genomic DNA was extracted from mouse tail biopsies using the Gentra Puregene Tissue Kit (Qiagen, Germantown, MD). A total of 48 overlapping pairs of amplicons (primers: F3gene_1-F3gene_35; upstreamF3_1-upstreamF3_13, Sup. Table 10) were used to Sanger sequence the entire *F3* gene (~11kb) and an additional ~5kb of upstream sequences on both strands. Sanger sequencing was performed at the University of Michigan Sequencing Core. For the analysis of candidate mutations, amplicons were generated harboring the nucleotide of interest using the outer primer pairs. Inner forward and reverse primers were used to bidirectionally sequence these amplicons. Sequencing chromatograms were visualized and manually scored using FinchTV.

Estimation of *F3* allelic expression

$F5^{L/L}$ $Tfpi^{+/-}$ mice with one B6 allele (in *cis* with ENU induced variants) and one 129S1 allele at the Chr3 candidate region were outcrossed to DBA wildtype females introducing exonic B6-129S1/DBA SNPs. Five progeny from this cross (2 B6/DBA and 3 129S1/DBA allele carriers, identified by DNA genotyping) were tested for differential allelic expression. From each mouse three tissue samples (lung, liver, whole brain) were obtained as previously described[22]. RNA was extracted from the tissue samples using RNeasy Plus Mini Kit (Qiagen) according to manufacturer's recommendations and reverse transcribed using SuperScript II (Invitrogen, Carlsbad, CA). cDNA corresponding to exon3-exon5 was amplified with primers F3-exon-F (5'TGCTTCTCGACCACAGACAC) and F3-exon-R (5'CTGCTTCCTGGGCTATTTTG), using

Gotaq Green Master Mix (Promega, Madison, WI). Primers F3-exon-F and F3-exon-R were also used to Sanger sequence the *F3* exonic region.

The *F3* exonic region harbors 3 known B6-129S1/DBA SNPs (rs30268372, rs30269285, rs30269288, http://www.ncbi.nlm.nih.gov/SNP/) that were used for relative expression analysis. Relative expression was estimated at SNP sites by dividing the area under the Sanger sequencing peak of one allele to another[46, 47]. Next, the relative expression of each SNP was compared between the B6 and 129S1 allele carrying progeny.

Mouse whole exome sequencing

Libraries were prepared using Agilent (Agilent Technologies, Santa Clara, CA) or NimbleGen (Roche NimbleGen, Madison, WI) mouse whole exome capture kits. 100 bp paired-end sequencing was performed on the Illumina Hiseq 2000 platform at the University of Michigan DNA Sequencing Core. A detailed overview of the whole exome sequencing pipeline is available at GitHub (https://github.com/tombergk/FVL_SUP). Briefly, sequence reads were aligned using Burrows-Wheeler Alignment software[48] to the mouse reference genome (genome assembly GRCm38, Ensembl release 73). Reads were sorted and duplications removed using Picard tools (http://picard.sourceforge.net). Coverage statistics were estimated using QualiMap software[49]. Variants were called across 8 samples using GATK HaplotypeCaller software[50]. Standard hard filters recommended by the Broad Institute were applied using GATK VariantFiltration[50] followed by an in-house developed pipeline to remove variants between the B6 and 129S1 strains, shared variants within our mouse cohort and variants in closer proximity than 200 base pairs from each other. Variants were annotated using Annovar software[51] with Refseq annotation (release 61). Heterozygous variants within exonic regions with >6X coverage unique for only one mouse in the cohort were regarded as potential ENU induced variants. A

total of 125 heterozygous variants were identified as candidate suppressor mutations, using an in-house filtering pipeline[46], with 79 variants occurring within coding sequence. The number of ENU variants identified in each exome sequenced mouse varied by genealogical distance from the G1 *MF5L* founder. The candidate ENU induced variants were validated by Sanger sequencing.

Generation of *Actr2* CRISPR/Cas9 targeted mice and cells

Actr2 Targeting Sequence Design and Cloning: CRISPR/Cas9 is widely used for genome editing. Cas9 is guided to a sequence specific cleavage site by small single-guide RNAs (sgRNA) through Watson-Crick base pairing with target DNA[52-54]. We obtained expression vectors for human-codon optimized *S. pyogenes* Cas9 and chimeric sgRNA (pSpCas9(BB); pX330; plasmid ID: 42230)[55] as well as the puromycin resistance gene for the selection of transfected cells (pSpCas9(BB)-2A-Puro; pX459; plasmid ID:48139)[56] from Addgene. Each vector was digested with *BbsI* and a pair of annealed oligos (sgRNA) was independently cloned into the backbone vector as described[56] and depicted in Sup. Fig 2.

The required *Actr2*-specific sgRNAs were selected based on: 1) their proximity to the mutation site (< 100 base-pair (bp) away; 10 bp optimal); 2) the presence of a protospacer adjacent motif (PAM) "NGG" sequence adjacent to the sgRNA; 3) the ability to incorporate a synonymous variant within the PAM to protect the homology directed repair (HDR) donor template from Cas9-targeted degradation; and 4) the sequence must have an inverse likelihood of off-target binding score of >70 and no less than 3 mismatches within exonic regions of the genome as determined by the CRISPR design tool (crispr.mit.edu).

Single-Stranded DNA Donor for Homology Directed Repair: The single-stranded DNA (ssDNA) oligo that served as an HDR donor template was ordered as an Ultramer DNA oligo

from Integrated DNA Technologies (IDT). This HDR donor template consists of a 161 bp genomic sequence homologous to a region spanning -44 to +117 bp from the splice junction of intron 6 and exon 7 of the mouse *Actr2* gene (Fig. 8B). This HDR donor encodes an arginine (R) to glycine (G) mutation at the 258th amino acid position (c.772C>G) and a synonymous mutation within the PAM to prevent donor DNA cleavage by Cas9. In this design, 80 bp homology arms flank the C to G transversion mutation with the position of the double-strand break (DSB) occurring 11 – 12 bp downstream of the homology arm junction for the sgRNA.

Mouse Pronuclear Injection for Validation of sgRNA and HDR Efficiency: Microinjection of CRISPR/Cas9 constructs into fertilized eggs and then analyzing blastocyst stage embryos for toxicity and efficacy is effective for ensuring that CRISPR design and reagent preparation have been carried out effectively. Blastocysts obtained just before implantation are suitable for testing the fidelity of CRIPSR/Cas9-mediated genome editing because they can be individually handled *in vitro* and obtained 3 days after microinjection[57]. The University of Michigan Transgenic Animal Model Core under the direction of Dr. Thomas Saunders has completed injection of 13 pronuclei and has grown them to the blastocyst stage.

Statistical Data Analysis

Statistical differences among the potential progeny of mouse crosses were determined using the X^2 test. The paired t-test was used for estimating statistical differences between the weights of $F5^{L/L}$ $Tfpi^{+/-}$ mice and their littermates. Relative expression differences for *F3* alleles were estimated using the Wilcoxon rank-sum test. Kaplan Meier analysis was used to assess significance for putative suppressors identified by exome sequencing. Probability of survival was calculated and plotted using Medcalc.

Acknowledgements

This research was supported by NIH grant P01-HL057346 (to D. Ginsburg). R.J. Westrick was generously supported by the following American Heart Association grants: Predoctoral Fellowship 0315212Z, Innovative Research Grant 10IRG3740035, and Scientist Development Grant 12SDG12140000. K. Tomberg is an International Fulbright Science and Technology Fellow and the recipient of an American Heart Association Predoctoral Fellowship Grant. A.E. Siebert is the recipient of an Oakland University Provost Award. M.A. Brake is the recipient of an American Heart Association Undergraduate Fellowship 15UFEL25700204. D. Ginsburg in an Investigator of the Howard Hughes Medical Institute. We gratefully acknowledge expertise of the Transgenic Animal Model Core of the University of Michigan's Biomedical Research Core Facilities for assistance with generating the *Actr2* CRISPR/Cas9 mice used in this study.

References

1. Silverstein MD, Heit JA, Mohr DN, Petterson TM, O'Fallon WM, Melton LJ, 3rd. Trends in the incidence of deep vein thrombosis and pulmonary embolism: A 25-year population-based study. *Arch Intern Med*. 1998;158:585-593
2. Souto JC, Almasy L, Borrell M, Gari M, Martinez E, Mateo J, Stone WH, Blangero J, Fontcuberta J. Genetic determinants of hemostasis phenotypes in spanish families. *Circulation*. 2000;101:1546-1551
3. Tregouet DA, Delluc A, Roche A, Derbois C, Olaso R, Germain M, de Andrade M, Tang W, Chasman DI, van Hylckama Vlieg A, Reitsma PH, Kabrhel C, Smith N, Morange PE. Is there still room for additional common susceptibility alleles for venous thromboembolism? *J Thromb Haemost*. 2016
4. Dentali F, Sironi AP, Ageno W, Turato S, Bonfanti C, Frattini F, Crestani S, Franchini M. Non-o blood type is the commonest genetic risk factor for vte: Results from a meta-analysis of the literature. *Semin Thromb Hemost*. 2012;38:535-548
5. Rosendaal FR, Reitsma PH. Genetics of venous thrombosis. *J Thromb Haemost*. 2009;7 Suppl 1:301-304
6. Dahlback B. Advances in understanding pathogenic mechanisms of thrombophilic disorders. *Blood*. 2008;112:19-27
7. Lijfering WM, Rosendaal FR, Cannegieter SC. Risk factors for venous thrombosis - current understanding from an epidemiological point of view. *Br J Haematol*. 2010;149:824-833
8. Westrick RJ, Ginsburg D. Modifier genes for disorders of thrombosis and hemostasis. *J Thromb Haemost*. 2009;7 Suppl 1:132-135
9. Recommendations from the egapp working group: Routine testing for factor v leiden (r506q) and prothrombin (20210g>a) mutations in adults with a history of idiopathic venous thromboembolism and their adult family members. *Genet Med*. 2011;13:67-76
10. De Stefano V, Martinelli I, Mannucci PM, Paciaroni K, Chiusolo P, Casorelli I, Rossi E, Leone G. The risk of recurrent deep venous thrombosis among heterozygous carriers of both factor v leiden and the g20210a prothrombin mutation. *N Engl J Med*. 1999;341:801-806
11. van Boven HH, Reitsma PH, Rosendaal FR, Bayston TA, Chowdhury V, Bauer KA, Scharrer I, Conard J, Lane DA. Factor v leiden (fv r506q) in families with inherited antithrombin deficiency. *Thromb Haemost*. 1996;75:417-421
12. Cui J, Eitzman DT, Westrick RJ, Christie PD, Xu ZJ, Yang AY, Purkayastha AA, Yang TL, Metz AL, Gallagher KP, Tyson JA, Rosenberg RD, Ginsburg D. Spontaneous thrombosis in mice carrying the factor v leiden mutation. *Blood*. 2000;96:4222-4226
13. Eitzman DT, Westrick RJ, Bi X, Manning SL, Wilkinson JE, Broze GJ, Ginsburg D. Lethal perinatal thrombosis in mice resulting from the interaction of tissue factor pathway inhibitor deficiency and factor v leiden. *Circulation*. 2002;105:2139-2142
14. Cordes SP. N-ethyl-n-nitrosourea mutagenesis: Boarding the mouse mutant express. *Microbiol Mol Biol Rev*. 2005;69:426-439
15. Moresco EM, Li X, Beutler B. Going forward with genetics: Recent technological advances and forward genetics in mice. *Am J Pathol*. 2013;182:1462-1473

16. Bull KR, Rimmer AJ, Siggs OM, Miosge LA, Roots CM, Enders A, Bertram EM, Crockford TL, Whittle B, Potter PK, Simon MM, Mallon AM, Brown SD, Beutler B, Goodnow CC, Lunter G, Cornall RJ. Unlocking the bottleneck in forward genetics using whole-genome sequencing and identity by descent to isolate causative mutations. *PLoS Genet*. 2013;9:e1003219
17. Buchovecky CM, Turley SD, Brown HM, Kyle SM, McDonald JG, Liu B, Pieper AA, Huang W, Katz DM, Russell DW, Shendure J, Justice MJ. A suppressor screen in mecp2 mutant mice implicates cholesterol metabolism in rett syndrome. *Nat Genet*. 2013;45:1013-1020
18. Tchekneva EE, Rinchik EM, Polosukhina D, Davis LS, Kadkina V, Mohamed Y, Dunn SR, Sharma K, Qi Z, Fogo AB, Breyer MD. A sensitized screen of n-ethyl-n-nitrosourea-mutagenized mice identifies dominant mutants predisposed to diabetic nephropathy. *J Am Soc Nephrol*. 2007;18:103-112
19. Matera I, Watkins-Chow DE, Loftus SK, Hou L, Incao A, Silver DL, Rivas C, Elliott EC, Baxter LL, Pavan WJ. A sensitized mutagenesis screen identifies gli3 as a modifier of sox10 neurocristopathy. *Hum Mol Genet*. 2008;17:2118-2131
20. Carpinelli MR, Hilton DJ, Metcalf D, Antonchuk JL, Hyland CD, Mifsud SL, Di Rago L, Hilton AA, Willson TA, Roberts AW, Ramsay RG, Nicola NA, Alexander WS. Suppressor screen in mpl-/- mice: C-myb mutation causes supraphysiological production of platelets in the absence of thrombopoietin signaling. *Proc Natl Acad Sci U S A*. 2004;101:6553-6558
21. Bank I, Libourel EJ, Middeldorp S, Hamulyak K, van Pampus EC, Koopman MM, Prins MH, van der Meer J, Buller HR. Elevated levels of fviii:C within families are associated with an increased risk for venous and arterial thrombosis. *J Thromb Haemost*. 2005;3:79-84
22. Nolan PM, Peters J, Strivens M, Rogers D, Hagan J, Spurr N, Gray IC, Vizor L, Brooker D, Whitehill E, Washbourne R, Hough T, Greenaway S, Hewitt M, Liu X, McCormack S, Pickford K, Selley R, Wells C, Tymowska-Lalanne Z, Roby P, Glenister P, Thornton C, Thaung C, Stevenson JA, Arkell R, Mburu P, Hardisty R, Kiernan A, Erven A, Steel KP, Voegeling S, Guenet JL, Nickols C, Sadri R, Nasse M, Isaacs A, Davies K, Browne M, Fisher EM, Martin J, Rastan S, Brown SD, Hunter J. A systematic, genome-wide, phenotype-driven mutagenesis programme for gene function studies in the mouse. *Nat Genet*. 2000;25:440-443
23. Justice MJ, Carpenter DA, Favor J, Neuhauser-Klaus A, Hrabe de Angelis M, Soewarto D, Moser A, Cordes S, Miller D, Chapman V, Weber JS, Rinchik EM, Hunsicker PR, Russell WL, Bode VC. Effects of enu dosage on mouse strains. *Mamm Genome*. 2000;11:484-488
24. Weber JS, Salinger A, Justice MJ. Optimal n-ethyl-n-nitrosourea (enu) doses for inbred mouse strains. *Genesis*. 2000;26:230-233
25. Lusis AJ. Genetics of atherosclerosis. *Trends Genet*. 2012;28:267-275
26. Yoo YJ, Mendell NR. The power and robustness of maximum lod score statistics. *Ann Hum Genet*. 2008;72:566-574
27. Kyrle PA, Minar E, Bialonczyk C, Hirschl M, Weltermann A, Eichinger S. The risk of recurrent venous thromboembolism in men and women. *N Engl J Med*. 2004;350:2558-2563

28. Roach RE, Lijfering WM, Tait RC, Baglin T, Kyrle PA, Cannegieter SC, Rosendaal FR. Sex difference in the risk of recurrent venous thrombosis: A detailed analysis in four european cohorts. *J Thromb Haemost*. 2015;13:1815-1822
29. Justice MJ, Noveroske JK, Weber JS, Zheng B, Bradley A. Mouse enu mutagenesis. *Hum Mol Genet*. 1999;8:1955-1963
30. Rotty JD, Wu C, Bear JE. New insights into the regulation and cellular functions of the arp2/3 complex. *Nat Rev Mol Cell Biol*. 2013;14:7-12
31. Vauti F, Prochnow BR, Freese E, Ramasamy SK, Ruiz P, Arnold HH. Arp3 is required during preimplantation development of the mouse embryo. *FEBS Lett*. 2007;581:5691-5697
32. Pollard TD, Beltzner CC. Structure and function of the arp2/3 complex. *Curr Opin Struct Biol*. 2002;12:768-774
33. Li Z, Kim ES, Bearer EL. Arp2/3 complex is required for actin polymerization during platelet shape change. *Blood*. 2002;99:4466-4474
34. Yang H, Wang H, Shivalila CS, Cheng AW, Shi L, Jaenisch R. One-step generation of mice carrying reporter and conditional alleles by crispr/cas-mediated genome engineering. *Cell*. 2013;154:1370-1379
35. Singh P, Schimenti JC, Bolcun-Filas E. A mouse geneticist's practical guide to crispr applications. *Genetics*. 2015;199:1-15
36. Morange PE, Suchon P, Tregouet DA. Genetics of venous thrombosis: Update in 2015. *Thromb Haemost*. 2015;114:910-919
37. Vineis P, Pearce N. Missing heritability in genome-wide association study research. *Nat Rev Genet*. 2010;11:589
38. Beutler B, Du X, Xia Y. Precis on forward genetics in mice. *Nat Immunol*. 2007;8:659-664
39. Gondo Y. Trends in large-scale mouse mutagenesis: From genetics to functional genomics. *Nat Rev Genet*. 2008;9:803-810
40. Simon MM, Moresco EM, Bull KR, Kumar S, Mallon AM, Beutler B, Potter PK. Current strategies for mutation detection in phenotype-driven screens utilising next generation sequencing. *Mamm Genome*. 2015;26:486-500
41. Toomey JR, Kratzer KE, Lasky NM, Stanton JJ, Broze GJ, Jr. Targeted disruption of the murine tissue factor gene results in embryonic lethality. *Blood*. 1996;88:1583-1587
42. Huang ZF, Higuchi D, Lasky N, Broze GJ, Jr. Tissue factor pathway inhibitor gene disruption produces intrauterine lethality in mice. *Blood*. 1997;90:944-951
43. Bi L, Lawler AM, Antonarakis SE, High KA, Gearhart JD, Kazazian HH, Jr. Targeted disruption of the mouse factor viii gene produces a model of haemophilia a. *Nat Genet*. 1995;10:119-121
44. Lange K, Papp JC, Sinsheimer JS, Sripracha R, Zhou H, Sobel EM. Mendel: The swiss army knife of genetic analysis programs. *Bioinformatics*. 2013;29:1568-1570
45. Lander E, Kruglyak L. Genetic dissection of complex traits: Guidelines for interpreting and reporting linkage results. *Nat Genet*. 1995;11:241-247
46. Tomberg K, Khoriaty R, Westrick RJ, Fairfield HE, Reinholdt LG, Brodsky GL, Davizon-Castillo P, Ginsburg D, Di Paola J. Spontaneous 8bp deletion in nbeal2 recapitulates the gray platelet syndrome in mice. *PLoS One*. 2016;11:e0150852

47. Mohlke KL, Purkayastha AA, Westrick RJ, Smith PL, Petryniak B, Lowe JB, Ginsburg D. Mvwf, a dominant modifier of murine von willebrand factor, results from altered lineage-specific expression of a glycosyltransferase. *Cell*. 1999;96:111-120
48. Li H, Durbin R. Fast and accurate short read alignment with burrows-wheeler transform. *Bioinformatics*. 2009;25:1754-1760
49. Garcia-Alcalde F, Okonechnikov K, Carbonell J, Cruz LM, Gotz S, Tarazona S, Dopazo J, Meyer TF, Conesa A. Qualimap: Evaluating next-generation sequencing alignment data. *Bioinformatics*. 2012;28:2678-2679
50. DePristo MA, Banks E, Poplin R, Garimella KV, Maguire JR, Hartl C, Philippakis AA, del Angel G, Rivas MA, Hanna M, McKenna A, Fennell TJ, Kernytsky AM, Sivachenko AY, Cibulskis K, Gabriel SB, Altshuler D, Daly MJ. A framework for variation discovery and genotyping using next-generation DNA sequencing data. *Nat Genet*. 2011;43:491-498
51. Wang K, Li M, Hakonarson H. Annovar: Functional annotation of genetic variants from high-throughput sequencing data. *Nucleic Acids Res*. 2010;38:e164
52. Jinek M, Chylinski K, Fonfara I, Hauer M, Doudna JA, Charpentier E. A programmable dual-rna-guided DNA endonuclease in adaptive bacterial immunity. *Science*. 2012;337:816-821
53. Garneau JE, Dupuis ME, Villion M, Romero DA, Barrangou R, Boyaval P, Fremaux C, Horvath P, Magadan AH, Moineau S. The crispr/cas bacterial immune system cleaves bacteriophage and plasmid DNA. *Nature*. 2010;468:67-71
54. Gasiunas G, Barrangou R, Horvath P, Siksnys V. Cas9-crrna ribonucleoprotein complex mediates specific DNA cleavage for adaptive immunity in bacteria. *Proceedings of the National Academy of Sciences of the United States of America*. 2012;109:E2579-2586
55. Cong L, Ran FA, Cox D, Lin S, Barretto R, Habib N, Hsu PD, Wu X, Jiang W, Marraffini LA, Zhang F. Multiplex genome engineering using crispr/cas systems. *Science*. 2013;339:819-823
56. Ran FA, Hsu PD, Wright J, Agarwala V, Scott DA, Zhang F. Genome engineering using the crispr-cas9 system. *Nature protocols*. 2013;8:2281-2308
57. Sakurai T, Watanabe S, Kamiyoshi A, Sato M, Shindo T. A single blastocyst assay optimized for detecting crispr/cas9 system-induced indel mutations in mice. *BMC Biotechnol*. 2014;14:69

Figure legends

Figure 1: ***F8* deficient thrombosuppression and design of the *Leiden* ENU mutagenesis screen. A.** The mating scheme and observed distributions of the $F5^{L/+}$ $Tfpi^{+/-}$ *F8* deficiency rescue experiments. *F8* X^{-} results in incompletely penetrant suppression of the $F5^{L/+}$ $Tfpi^{+/-}$ phenotype. **B.** The mating scheme and observed distribution of the *Leiden* screen. $F5^{L/+}$ $Tfpi^{+/-}$ male mice were mutagenized with either 1 x 150mg/kg or 3 x 90 mg/kg ENU and bred with non-mutagenized $F5^{L/L}$ females. Sixteen and 83 $F5^{L/L}$ $Tfpi^{+/-}$ progeny, respectively were observed in each of the dosing regimens, with over twice the rate of $F5^{L/L}$ $Tfpi^{+/-}$ survivors in the progeny of the 3 x 90 mg/kg treated mice. **C.** Though a trend toward worse survival among female $F5^{L/L}$ $Tfpi^{+/-}$ putative suppressor mice, this difference was not significant (p=0.114). **D and E.** $F5^{L/L}$ $Tfpi^{+/-}$ putative suppressor mice were significantly smaller than their non-$F5^{L/L}$ $Tfpi^{+/-}$ littermates in both the pure B6 and mixed B6-129S1 genetic backgrounds.

Figure 2: **The MF5L6 suppressor locus maps to Chr 3. A.** Linkage analysis for the MF5L6 line. The Chr 2 locus (LOD score=9.81) includes the *Tfpi* gene. The Chr 3 peak had the highest LOD score in the Chr3 subregion:117.3-124.8Mb (maximum LOD=4.49, 1 LOD interval). The most significant linkage signal (Chr 2, LOD score=9.81) spans the *Tfpi* locus and was generated by markers tightly linked to the $Tfpi^{-}$ allele. Due to the backcross history of our *Tfpi* mouse colony, these mice have a complicated *Tfpi* congenic interval containing 129S1 and B6 alleles linked to the knockout allele. Since these alleles are "passenger alleles", they will always be heterozygous as a result of our mating strategy (van vlijmen ref). **B.** The mating scheme and observed distribution of offspring to test *F3* deficiency as a suppressor of $F5^{L/+}$ $Tfpi^{+/-}$. $F3^{+/-}$ results in incompletely penetrant suppression of the $F5^{L/+}$ $Tfpi^{+/-}$ phenotype. **C.** The Chr 3 candidate interval (chr3:117.3-124.8 Mb) contains 38 refseq annotated genes, including *F3*.

Figure 3: **Discovery and validation of *Actr2* R258G as a thrombosis suppressor gene by NGS. A.** Kaplan-Meier survival plot for $F5^{L/L}$ $Tfpi^{+/-}$ mice with and without the *Actr2* mutation. $F5^{L/L}$ $Tfpi^{+/-}$ $Actr2^{+/G}$ exhibit significantly better survival than $F5^{L/L}$ $Tfpi^{+/-}$ $Actr2^{+/+}$ (n = 35 mice). **B.** ARP2 amino acid R258 is highly conserved in animals, plants and fungi.

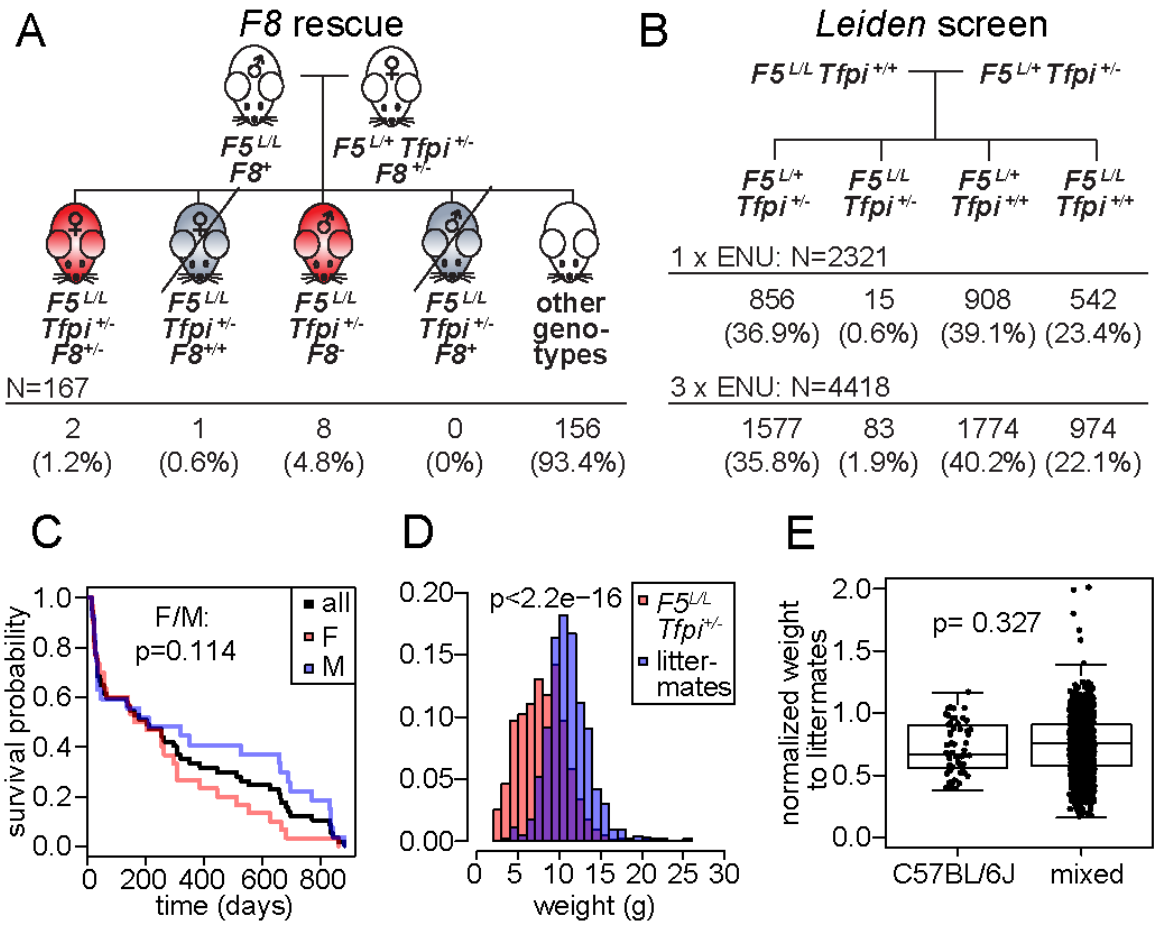

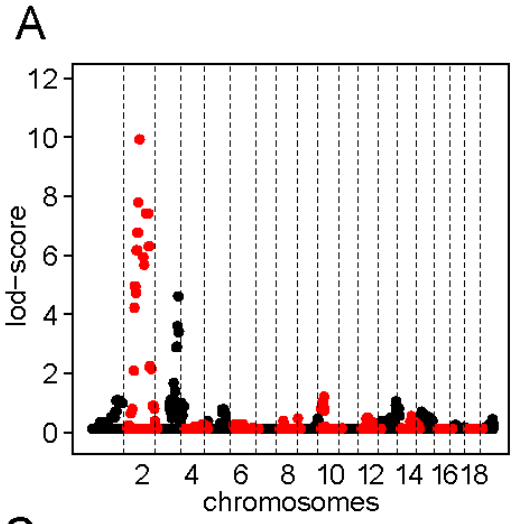

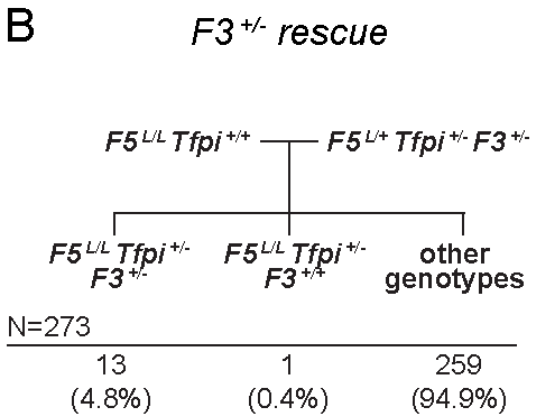

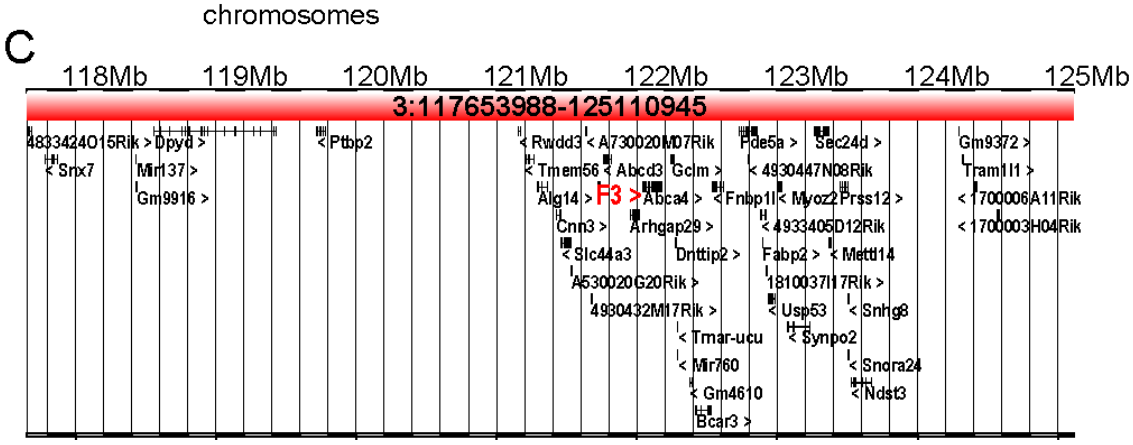

A

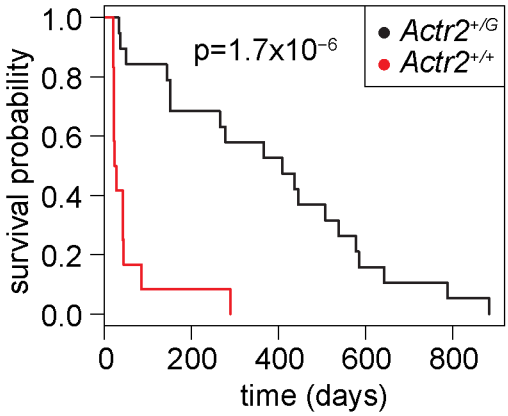

B